First publ. in: Journal of the American Chemical Society 129 (2007), 46, pp. 14362-14366

Single-Molecule Magnets: A New Approach To Investigate the Electronic Structure of Mn_{12} Molecules by Scanning Tunneling Spectroscopy

Michael Burgert,*,† Sönke Voss,‡ Simon Herr,‡ Mikhail Fonin,‡ Ulrich Groth,† and Ulrich Rüdiger‡

Contribution from the Fachbereich Chemie and Fachbereich Physik, Universität Konstanz, Universitätsstrasse 10, 78457 Konstanz, Germany

Abstract: A new approach to the deposition of Mn_{12} single-molecule magnet monolayers on the functionalized Au(111) surface optimized for the investigation by means of scanning tunneling spectroscopy was developed. To demonstrate this method, the new Mn_{12} complex $[Mn_{12}O_{12}(O_2CC_6H_4F)_{16}(EtOH)_4]\cdot 4.4CHCl_3$ was synthesized and characterized. In MALDI-TOF mass spectra the isotopic distribution of the molecular ion peak of the latter complex was revealed. The complex was grafted to Au(111) surfaces via two different short conducting linker molecules. The Mn_{12} molecules deposited on the functionalized surface were characterized by means of scanning tunneling microscopy showing homogeneous monolayers of highest quality. Scanning tunneling spectroscopy measurements over a wider energy range compared with previous results could be performed because of the optimized Au(111) surface functionalization. Furthermore, the results substantiate the general suitability of short acidic linker molecules for the preparation of Mn_{12} monolayers via ligand exchange and represent a crucial step toward addressing the magnetic properties of individual Mn_{12} single-molecule magnets.

Introduction

In the last two decades single-molecule magnets[1] (SMMs) have attracted much attention because of their unique magnetic properties such as quantum tunneling of magnetization[2] (QTM) and hysteresis of pure molecular origin[3] making them potential candidates for future applications as basic units in information technology devices.[4] The most widely investigated and first discovered[5] SMM is "Mn_{12} acetate"[6] (**1**) which allows for the tailoring of the ligand shell thus facilitating the synthesis of a broad variety of derivatives.[7] To date, experiments on the magnetic and electronic properties of SMMs have been performed mostly on crystals and powders[8−11] while the magnetic as well as the electronic properties of individual molecules or SMM monolayers on surfaces remain to a large extent unknown. Two possible experimental approaches to the investigation of the fundamental physical properties of individual Mn_{12} molecules are feasible: transport measurements in a single-molecule transistor geometry[12−15] or scanning tunneling spectroscopy (STS). For STS investigations, Mn_{12} complexes must be grafted to an appropriate surface. Recently, several different approaches to this goal have been reported, such as direct deposition of Mn_{12} complexes via sulfur containing ligands,[16−19] bonding of Mn_{12} complexes to functionalized Au(111) or Si(100) surfaces via ligand-exchange reaction,[20−22] or deposition of Mn_{12}

† Fachbereich Chemie.
‡ Fachbereich Physik.

(1) Christou, G.; Gatteschi, D.; Hendrickson, D. N.; Sessoli, R. *MRS Bull.* **2000**, *25*, 66.
(2) del Barco, E.; Kent, A. D.; Hill, S.; North, J. M.; Dalal, N. S.; Rumberger, E. M.; Hendrickson, D. N.; Chakov, N.; Christou, G. J. *Low Temp. Phys.* **2005**, *140*, 119.
(3) Sessoli, R.; Gatteschi, D.; Caneschi, A.; Novak, M. A. *Nature* **1993**, *365*, 141.
(4) Leuenberger, M. N.; Loss, D. *Nature* **2001**, *410*, 789.
(5) Caneschi, A.; Gatteschi, D.; Sessoli, R.; Barra, A. L.; Brunel, L. C.; Guillot, M. *J. Am. Chem. Soc.* **1991**, *113*, 5873.
(6) Lis, T. *Acta Crystallogr., Sect. B: Struct. Crystallogr. Cryst. Chem.* **1980**, *36*, 2042.
(7) Gatteschi, D.; Sessoli, R. *Angew. Chem.* **2003**, *115*, 278; *Angew. Chem., Int. Ed.* **2003**, *42*, 268.
(8) Sessoli, R.; Tsai, H.-L.; Schake, A. R.; Wang, S.; Vincent, J. B.; Folting, K.; Gatteschi, D.; Christou, G.; Hendrickson, D. N. *J. Am. Chem. Soc.* **1993**, *115*, 1804.
(9) Friedman, J. R.; Sarachik, M. P.; Tejada, J.; Ziolo, R. *Phys. Rev. Lett.* **1996**, *76*, 3830.
(10) Thomas, L.; Lionti, F.; Ballou, R.; Gatteschi, D.; Sessoli, R.; Barbara, B. *Nature* **1996**, *383*, 145.
(11) Wernsdorfer, W.; Murugesu, M.; Christou, G. *Phys. Rev. Lett.* **2006**, *96*, 057208.
(12) Heersche, H. B.; de Groot, Z.; Folk, J. A.; van der Zant, H. S. J.; Romeike, C.; Wegewijs, M. R.; Zobbi, L.; Barreca, D.; Tondello, E.; Cornia, A. *Phys. Rev. Lett.* **2006**, *96*, 206801.
(13) Jo, M.-H.; Grose, J. E.; Baheti, K.; Deshmukh, M. M.; Sokol, J. J.; Rumberger, E. M.; Hendrickson, D. N.; Long, J. R.; Park, H.; Ralph, D. C. *Nano Lett.* **2006**, *6*, 2014.
(14) Ni, C.; Shah, S.; Hendrickson, D.; Bandaru, P. R. *Appl. Phys. Lett.* **2006**, *89*, 212104.
(15) Henderson, J. J.; Ramsey, C. M.; del Barco, E.; Mishra, A.; Christou, G. *J. Appl. Phys.* **2007**, *101*, 09E102.
(16) Mannini, M.; Bonacchi, D.; Zobbi, L.; Piras, F. M.; Speets, E. A.; Caneschi, A.; Cornia, A.; Magnani, A.; Ravoo, B. J.; Reinhoudt, D. N.; Sessoli, R.; Gatteschi, D. *Nano Lett.* **2005**, *5*, 1435.
(17) Cornia, A.; Fabretti, A. C.; Pacchioni, M.; Zobbi, L.; Bonacchi, D.; Caneschi, A.; Gatteschi, D.; Biagi, R.; del Pennino, U.; De Renzi, V.; Gurevich, L.; van der Zant, H. S. J. *Angew. Chem., Int. Ed.* **2003**, *42*, 1645.
(18) Zobbi, L.; Mannini, M.; Pacchioni, M.; Chastanet, G.; Bonacchi, D.; Zanardi, C.; Biagi, R.; del Pennino, U.; Gatteschi, D.; Cornia, A.; Sessoli, R. *Chem. Commun.* **2005**, 1640.
(19) del Pennino, U.; De Renzi, V.; Biagi, R.; Corradini, V.; Zobbi, L.; Cornia, A.; Gatteschi, D.; Bondino, F.; Magnano, E.; Zangrando, M.; Zacchigna, M.; Lichtenstein, A.; Boukhvalov, D. W. *Surf. Sci.* **2006**, *600*, 4185.

molecules on a functionalized Au(111) surface via electrostatic interactions.[23] In a recent study[24] the direct deposition of a Mn_{12} complex via sulfur-containing ligands on the bare Au(111) surface was compared with the bonding of the same Mn_{12} complex to a functionalized Au(111) surface via ligand exchange reaction. In the case of direct deposition the complete destruction of Mn_{12} clusters due to the strong gold−sulfur interaction was revealed. However, for Mn_{12} clusters on the functionalized Au(111) surface the integrity of the Mn_{12} core could be substantiated by means of X-ray absorption spectroscopy and X-ray photoemission.[24]

In this paper we present a method that allows for a reliable deposition and investigation of a broad variety of Mn_{12} derivatives on the functionalized Au(111) surface using short acidic highly conductive linker molecules giving a possibility to investigate the electronic structure of the deposited SMMs by STS. In contrast to previous publications in which a very flexible linker molecule (16-mercaptohexadecanoic acid) was used to functionalize the Au(111) surface,[20] we did not focus our interest on the sterical aspects of the ligand exchange reaction. This ligand exchange reaction of Mn_{12} is a chemical equilibrium which is driven to completion by using a more acidic carboxylic acid for substitution than the replaced carboxylic acid. For a successful ligand exchange reaction we postulated that the pK_a difference is more important than the flexibility of the linker molecule. Furthermore for STS investigations linker molecules should be short and should ensure an appropriate electronic coupling between the Mn_{12} complex and the Au(111) surface.[25] To this end, alkanes with long saturated chains are known to exhibit a lower conductivity[26] while the molecules with delocalized π-electrons should be more suitable because of their conductor-like behavior in STS experiments.[27] All of these conditions are fulfilled by the linker molecules used in the present experiments: 4′-mercapto-octafluorobiphenyl-4-carboxylic acid (4-MOBCA) and 4-mercapto-2,3,5,6-tetrafluorobenzoic acid (4-MTBA). To demonstrate our method we describe the synthesis and the characterization of the new Mn_{12} compound $[Mn_{12}O_{12}(O_2CC_6H_4F)_{16}(EtOH)_4]$ (**2**)·$4.4CHCl_3$ first and present details of its deposition on the Au(111) surfaces functionalized by 4-MOBCA as well as 4-MTBA afterward. Furthermore, we present the investigation of the electronic structure of **2** grafted on the functionalized Au(111) surfaces by means of room-temperature ultrahigh vacuum STS.

Experimental Section

Compound Preparation. All chemicals and solvents were used as received. $[Mn_{12}O_{12}(O_2CCH_3)_{16}(H_2O)_4]$ (Mn_{12}ac)[6] (**1**) and 4-mercapto-2,3,5,6-tetrafluorobenzoic acid[32] were prepared as described elsewhere. Details of the synthesis and the characterization of 4′-mercapto-octafluorobiphenyl-4-carboxylic acid are given in the Supporting Information.

$[Mn_{12}O_{12}(O_2CC_6H_4F)_{16}(EtOH)_4]$ (2)·$4.4CHCl_3$. A slurry of **1** (0.5 g, 0.24 mmol) in a solution of *p*-fluorobenzoic acid (0.82 g, 5.8 mmol) in CH_2Cl_2 (60 mL) was stirred overnight, and the solvent was evaporated under reduced pressure. Toluene (30 mL) was added to the residue to remove acetic acid, and the solution was again evaporated. The addition and removal of CH_2Cl_2 and toluene was repeated three more times. The remaining solid was redissolved in CH_2Cl_2 (70 mL) and filtered through kieselguhr. An equal volume of hexane was added, and the solution was allowed to stand undisturbed at 4 °C for 3 days. The resulting black crystals were collected by filtration, washed with hexane, and dried in vacuo. A crystallography sample was grown slowly from $CHCl_3$ solution covered with hexane at 4 °C in 3 weeks and maintained in mother liquor to avoid solvent loss. Anal. Calcd (found) for dried $C_{112}H_{72}F_{16}Mn_{12}O_{48}$: C, 42.72 (42.69); H, 2.30 (2.22). Selected IR bands (KBr pellet, cm^{-1}): 1606 (s), 1506 (m), 1420 (vs), 1352 (m), 1233 (m), 1149 (m), 852 (m), 782 (m), 624 (m, br). MALDI-TOF−MS (*m*/*z*): 3076.5 $\{[Mn_{12}O_{12}(O_2CC_6H_4F)_{16}]\}^+$; 2937.5 $\{[Mn_{12}O_{12}(O_2CC_6H_4F)_{15}]\}^+$; 2798.4 $\{[Mn_{12}O_{12}(O_2CC_6H_4F)_{14}]\}^+$.

X-ray Crystallography. Crystal data for **2**: $C_{123.73}H_{82.40}Cl_{13.03}F_{16}Mn_{12}O_{48}$, $M_r = 3762.12$, orthorhombic, *Pna*21, $a = 17.9874(4)$ Å, $b = 25.3631(5)$ Å, $c = 32.8163(5)$ Å, $V = 14971.3(5)$ Å^3, $T = 100$ K, $Z = 4$, ρ_{calcd} (g/cm^3) = 1.669, 260504 reflections collected, 37570 unique ($R_{int} = 0.162$), $R_1 = 0.0580$, $wR_2 = 0.1354$, using 19439 reflections with $I > 2\sigma(I)$ to refine 1971 parameters. The data collection was performed at a STOE IPDS−II diffractometer equipped with a graphite monochromated radiation source ($\lambda = 0.71073$ Å) and an image plate detection system. The selection, integration, and averaging procedure of the measured reflex intensities, the determination of the unit cell by a least-squares fit of the 2Θ values, data reduction, LP correction, and the space group determination were performed using the X-Area software package delivered with the diffractometer. A semiempirical absorption correction method was performed after indexing of the crystal faces. The structure was solved by direct methods (SHELXS-97)[33] and standard Fourier techniques against F^2 with a full-matrix least-squares algorithm using SHELXL-97 and the WinGX (1.70)[34] software package. All non-hydrogen atoms were refined anisotropically. Hydrogen atoms were placed in calculated positions and refined with a riding model. Because of the noncentrosymmetric space group and a Flack parameter about 0.532 an absolute structure refinement was performed using the SHELX-97 TWIN instruction. One *p*-fluorobenzoate molecule is disordered over two positions, whose site occupancy factors were dependently refined to 70:30%. Because of the weak occupancy of the second position the participating ethanol molecule could not be localized. Five chloroform molecules could be found in the solvent accessible voids of the structure. The occupancy factors of four chloroform molecules were determined to 100%, of one chloroform molecule to 40%. Several Cl atoms have to be split in two parts because of the strong disorder of the chloroform molecules.

Physical Measurements. C, H elemental analysis was carried out in a Heraeus CHN−O rapid analyzer on samples recrystallized from

(20) Naitabdi, A.; Bucher, J.-P.; Gerbier, P.; Rabu, P.; Drillon, M. *Adv. Mater.* **2005**, *17*, 1612.
(21) Fleury, B.; Catala, L.; Huc, V.; David, C.; Zhong, W. Z.; Jegou, P.; Baraton, L.; Palacin, S.; Albouy, P.-A.; Mallah, T. *Chem. Commun.* **2005**, 2020.
(22) Condorelli, G. G.; Motta, A.; Fragalà, I. L.; Giannazzo, F.; Raineri, V.; Caneschi, A.; Gatteschi, D. *Angew. Chem., Int. Ed.* **2004**, *43*, 4081.
(23) Coronado, E.; Forment-Aliaga, A.; Romero, F. M.; Corradini, V.; Biagi, R. De Renzi, V.; Gambardella, A.; del Pennino, U. *Inorg. Chem.* **2005**, *44*, 7693.
(24) Voss, S.; Fonin, M.; Rüdiger, U.; Burgert, M.; Groth, U.; Dedkov, Y. S. *Phys. Rev. B* **2007**, *75*, 045102.
(25) Voss, S.; Fonin, M.; Rüdiger, U.; Burgert, M.; Groth, U. *Appl. Phys. Lett.* **2007**, *90*, 133104.
(26) Labonté, A. P.; Tripp, S. L.; Reifenberger, R.; Wei, A. *J. Phys. Chem. B* **2002**, *106*, 8721.
(27) Rosink, J. J. W. M.; Blauw, M. A.; Geerligs, L. J.; van der Drift, E.; Radelaar, S. *Phys. Rev. B* **2000**, *62*, 10459.
(28) Mercury: visualization and analysis of crystal structures. Macrae, C. F.; Edgington, P. R.; McCabe, P.; Pidcock, E.; Shields, G. P.; Taylor, R.; Towler, M.; van de Streek, J. *J. Appl. Cryst.* **2006**, *39*, 453.
(29) Boukhvalov, D. W.; Al-Saqer, M.; Kurmaev, E. Z.; Moewes, A.; Galakhov, V. R.; Finkelstein, L. D.; Chiuzbaian, S.; Neumann, M.; Dobrovitski, V. V.; Katsnelson, M. I.; Lichtenstein, A. I.; Harmon, B. N.; Endo, K.; North, J. M.; Dalal, N. S. *Phys. Rev. B* **2007**, *75*, 014419.
(30) North, J. M.; Zipse, D.; Dalal, N. S.; Choi, E. S.; Jobiliong, E.; Brooks, J. S.; Eaton, D. L. *Phys. Rev. B* **2003**, *67*, 174407.
(31) Oppenheimer, S. M.; Sushkov, A. B.; Musfeldt, J. L.; Achey, R. M.; Dalal, N. S. *Phys. Rev. B* **2002**, *65*, 054419.
(32) Tamborski, C.; Soloski, E. J. *J. Org. Chem.* **1966**, *31*, 746.
(33) Sheldrick, G. M. S*HELX-97, an integrated system for solving and refining crystal structures from diffraction data*; University of Göttingen: Göttingen, Germany, 1997.
(34) Farrugia, L. J. *J. Appl. Crystallogr.* **1999**, *32*, 837.

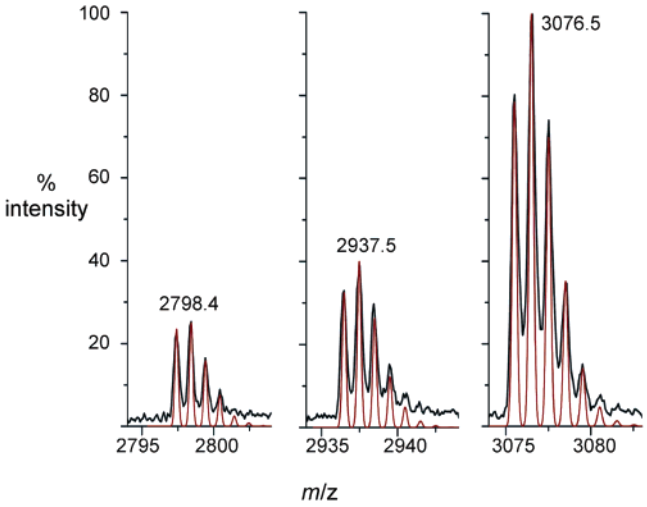

Figure 1. Measured (black) and calculated (red) isotopic distribution of $[M]^+$, $[M - L]^+$ and $[M - 2L]^+$ of **2** in positive, reflector MALDI-TOF spectrum.

CH_2Cl_2 and dried in vacuo. IR transmission spectra were recorded at room temperature in a Perkin-Elmer 1600 FT-IR spectrometer. MALDI-TOF mass spectra were recorded on a Bruker Biflex III spectrometer in the positive, reflector mode with a delayed extraction MALDI source and a pulsed nitrogen laser (337 nm). The sample was prepared by mixing a solution of **2**·4.4$CHCl_3$ in $CHCl_3$ (3 μL, 10 mg/mL) with a solution of the matrix in $CHCl_3$ (*trans*-2-[3-(4-*tert*-butylphenyl)-2-methyl-2-propenylidene]malononitrile, 10 μL, 30 mg/mL). A 0.8 μL-aliquot of the mixture was placed on the target plate, evaporated in air, and transferred to the mass spectrometer for analysis. A Quantum Design MPMS XL5 system was used to perform magnetic measurements.

The Au(111) single crystal was Ar+ sputtered at 800 eV and annealed to 600 °C. 2 mM 4-mercapto-2,3,5,6-tetrafluorobenzoic acid (4-MTBA) solution in ethanol (5 min) and 2 mM 4-mercapto-octafluorobiphenyl-4′-carboxylic acid (4-MOBCA) solution in ethanol were used for functionalization of the Au surface. The Au(111) single crystal was rinsed thoroughly with ethanol and dichloromethane. After drying with N_2 the functionalized crystal was immersed in a 0.04 mM solution of **2** for 10 min and dried carefully under strict exclusion of water. We found that only samples prepared from carefully selected single crystals were suited for a reliable deposition. The samples were introduced into the ultrahigh vacuum (UHV) chambers via ultrafast load locks to avoid surface contaminations. STM, STS, and XPS measurements were performed with an Omicron Multiprobe UHV system (base pressure 10^{-11} mbar) at room temperature. In all STM experiments performed with the Omicron VT AFM/STM electrochemically etched tungsten tips, flash-annealed by electron bombardment were used. Scanning parameters for the images shown in Figure 4a and 4c were $U_T = 1$ V and $I_T = 6.9$ pA; in Figure 4b and 4d $U_T = 2$ V and $I_T = 6.9$ pA. XPS spectra were collected using the nonmonochromatized Al Kα (1486.6 eV) line. The energy resolution of the Omicron EA 125 analyzer was set to 0.65 eV full width at half-maximum.

Results and Discussion

MALDI-TOF Mass Spectrometry. Mass spectra collected in positive reflector mode show signals at $m/z = 3076.5$, 2937.5, and 2798.4 that correspond to the cluster ion $[M]^+ = \{[Mn_{12}O_{12}L_{16}]\}^+$ (with L = $O_2CC_6H_4F$) and its fragments $[M\text{-}L]^+$ and $[M\text{-}2L]^+$ (Figure 1). The ethanol molecules are lost under the experimental conditions. We present the isotopic distribution of the $[M]^+$, $[M\text{-}L]^+$, and $[M\text{-}2L]^+$ signal in the positive reflector mode. The exact determination of the masses

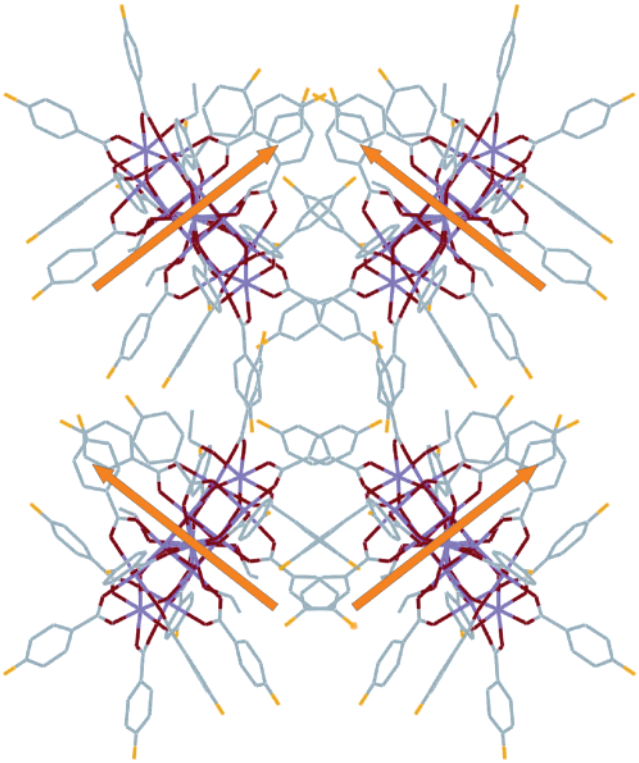

Figure 2. Plot of **2**·4.4$CHCl_3$ (solvent and hydrogens removed).[28] The view along the *a*-axis reveals two different orientations of the easy axes (denoted by arrows) of the Mn_{12} cores: Mn, purple; O, red; C, gray; F, green.

shows that the cluster ions are not produced by taking a proton from the matrix. In our opinion the ions are created by redox processes during crystallization under aerobic conditions or by electron transfer from matrix molecules coordinated immediately to the Mn_{12} complex during laser irradiation.

X-ray Structure of $[Mn_{12}O_{12}(O_2CC_6H_4F)_{16}(EtOH)_4]$ (2)·4.4$CHCl_3$. The complex crystallizes in the noncentrosymmetric space group *Pna*21 with the composition **2**·4.4 $CHCl_3$. The structure of the $[Mn_{12}O_{12}]^{16+}$ core is similar to other Mn_{12} complexes. The central $[Mn_4^{IV}O_4]^{8+}$ cubane is surrounded by a ring of eight Mn^{III} ions that are held together via eight μ_3-O_2- ions. The residual free sites of the manganese ions are occupied with eight axial and eight equatorial μ_2-bridging *p*-fluorobenzoate molecules and four ethanol molecules. Complex **2**·4.4$CHCl_3$ was crystallized from chloroform that contains 1% ethanol for stabilization. The H_2O molecules being usually present in Mn_{12} complexes are replaced by ethanol during the three-week crystallization time. The packing of the molecules in the crystal (Figure 2) differs from most known Mn_{12} complexes and reveals two species of complex **2** with different orientations of the easy axes of the Mn_{12} cores that are nearly perpendicular to each other.

Magnetic Measurements. The SMM character of complex **2**·4.4$CHCl_3$ was confirmed by SQUID magnetometry measurements in the 1.7−2.3 K range (Figure 3). The hysteresis loops show the characteristic steps, separated by plateaus, indicating QTM. The slight broadening of the steps is due to the different orientation of the easy axes of the two molecular species within the single crystal resulting in transverse field components. From all characterizing data above we conclude that compound **2**·4.4$CHCl_3$ is a new member of the SMM Mn_{12} family.

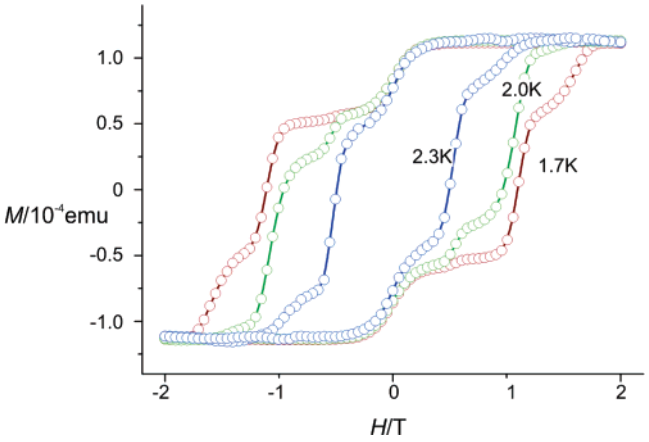

Figure 3. Measurement of magnetization **M** versus magnetic field **H** (d**H**/dt = 0.001 T/s) applied along the crystallographic b-axis of a single crystal of **2**·4.4$CHCl_3$.

Surface Preparation and Characterization. For the preparation of the functionalized Au(111) surface a gold single crystal was dipped into a solution of 4-MOBCA or 4-MTBA. Since complex **2** will be reduced to Mn^{II} fragments by free thiol groups,[17] the Au(111) surface was rinsed thoroughly with ethanol and dichloromethane to clean it from residual acid. After the Au(111) surface was immersed in the 4-MOBCA (4-MTBA) solution the typical Au(111) surface reconstruction is no more visible (Figure 4a and 4c). X-ray photoelectron spectroscopy (XPS) shows the presence of fluorine and carbon signals confirming the successful deposition (see Supporting Information). For the deposition of complex **2** via the ligand-exchange reaction the functionalized Au(111) single-crystal surface was dipped into a solution of **2** in dichloromethane. Complex **2** used for preparation was of highest crystalline quality. Even a small amount of Mn^{II} and Mn^{III} fragments remaining from synthesis leads to the passivation of carboxylic groups on the Au surface preventing the deposition of **2**. In this case flat clusters with an average height of 0.1−0.3 nm were visible in STM images and a weak Mn 2p peak in XPS spectra was observed, although no intact Mn_{12} molecules were grafted on the surface. In the case of successful deposition a very homogeneous and dense layer of clusters could be detected by STM (Figure 4b and 4d). The deposited Mn_{12} clusters have a diameter of 2.4 ± 0.2 nm full width at half-maximum and an average height of 1.2 ± 0.1 nm. The apparent diameter of the molecules is slightly larger than the expected diameter of about 2 nm derived from the crystal structure; that can be explained by the apex geometry of the STM tip used in this experiment. In addition, Mn_{12} clusters deposited on the functionalized Au(111) surface could not be moved by the STM tip across the surface during scanning that indicates a successful chemisorption of the Mn_{12} clusters.

To substantiate the thesis of the ligand exchange mechanism we prepared a monolayer of 2,3,5,6-tetrafluorothiophenol on the Au(111) surface and tried to deposit Mn_{12} complexes from dichloromethane solution. In STM images, which were comparable with those in Figure 4a and 4c, no hints for the deposition of **2** could be found. In XPS only a very weak Mn 2p signal indicating traces of adsorbed manganese impurities was observed. A second test regarding the stability of the monolayer and the ligand exchange reaction in the presence of solvent was performed by treating the monolayer of Mn_{12} molecules deposited on the functionalized Au(111) surface with

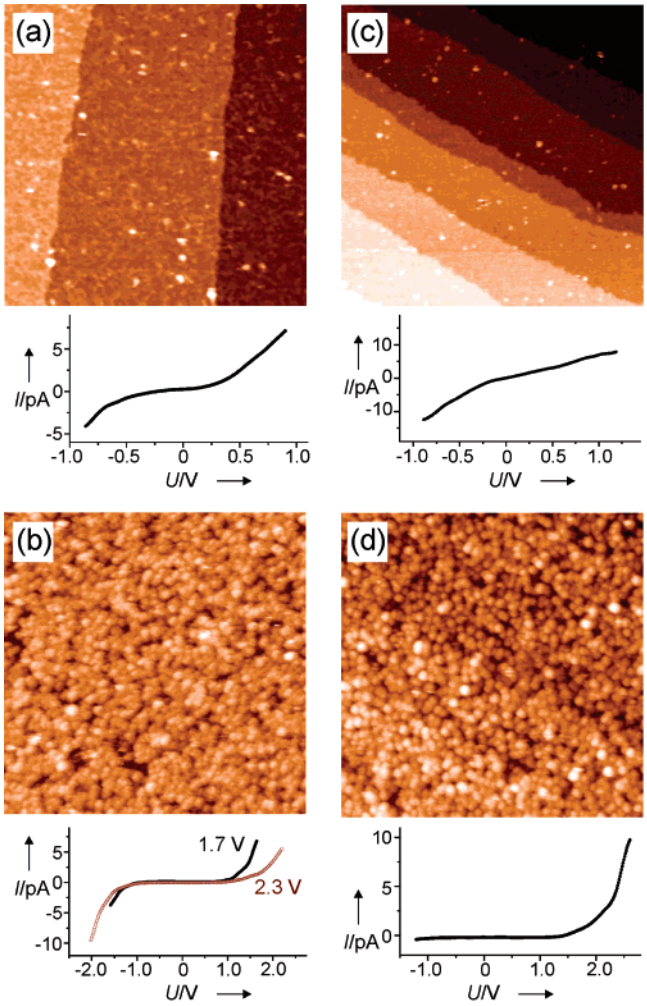

Figure 4. 150 × 150 nm^2 STM images of (a) the 4-MOBCA functionalized surface, (b) compound **2** deposited on the 4-MOBCA functionalized Au(111) surface, (c) the 4-MTBA functionalized surface, and (d) compound **2** deposited on the 4-MTBA functionalized Au(111) surface. Lower panels of graphics a and c show the corresponding $I-U$ characteristics for each functionalized surface. Lower panels of graphics b and d show the corresponding $I-U$ curves measured on top of the Mn_{12} clusters. In the lower panel of graphic b two $I-U$ curves are presented corresponding to different set voltages (1.7 and 2.3 V) used in the measurements.

solutions of carboxylic acids in dichloromethane for 5 min. STM and XPS measurements showed that all Mn_{12} molecules were removed from the functionalized surface. These results indicate that the ligand-exchange reaction with the functionalization layer is a highly dynamic and gentle process that permanently occurs in solution. Hence, a "snapshot" of the process seems to be generated when the sample is removed from the solvent.

Scanning Tunneling Spectroscopy. Along with the STM images of Mn_{12} monolayers we also performed STS measurements on individual Mn_{12} clusters grafted on the functionalized Au(111) surface. Lower panels of Figure 4 show $I-U$ characteristics recorded on the 4-MOBCA (a) and on the 4-MTBA (c) functionalized Au(111) surface as well as at the center of the molecules **2** deposited on the 4-MOBCA (b) and 4-MTBA (d). The $I-U$ curves presented in this work were obtained by averaging over at least 30 (4-MOBCA) or 6 (4-MTBA) curves taken at different locations of the sample surface. The $I-U$ characteristics taken on the functionalized surfaces (Figure 4a and 4c) show the features typical for aromatic thiols with an asymmetry between positive and negative bias voltages.[27]

Both $I-U$ curves obtained at the center of compound **2** clusters deposited on the 4-MOBCA functionalized Au surface show a line shape revealing a broad region of low conductivity. In case of compound **2** deposited on the 4-MTBA functionalized surface (Figure 4d) we found that increasing the bias voltage beyond −1.2 V during STS measurements leads to large instabilities in the $I-U$ spectra. In contrast to 4-MTBA, the use of 4-MOBCA was found to be more advantageous since no instabilities in the STS spectra in both positive and negative bias voltage ranges were observed. This allows for the investigation of a broader energetic region near the Fermi energy compared with the previous studies.[25] Moreover, STS measurements at different set voltages were possible on **2** deposited on the 4-MOBCA functionalized Au(111) surface (see Figure 4b). The $I-U$ characteristics in the region of the positive bias voltage (Figure 4b) are comparable to that presented in Figure 4d showing a slightly smaller region of low conductivity. The width of the latter region was determined to be about 2 eV (Figure 4b) that is close to the value measured for another Mn_{12} derivative bound to the Au(111) surface.[25] The STS spectrum obtained at a set voltage of 1.7 V (Figure 4b) is nearly symmetric. This symmetry indicates that the electrostatic coupling between molecule and substrate is comparable to the coupling between tip and molecule.[26] In previous studies this condition was used to estimate the E_F-HOMO difference, which is one-fourth of the measured energy gap width.[26] Assuming a negligible contribution from the ligands as well as from the linker molecules because of their expected conductor-like behavior in STS measurements, application of this formalism to compound **2** yields a value of 0.5 ± 0.2 eV. This value would be in reasonable agreement with the electronic structure found in the combined experimental and theoretical study of Mn_{12}-acetate.[29] In the latter study the experimental spectroscopic data was compared with electronic structure calculations in the frame of local density approximation taking into account the on-site Coulomb interaction (LDA + U) and was found to be in good agreement with the experimental spectra for $U = 4$ eV which also delivers reasonable values for the energy gap.[29] On the other hand, in the different optical studies the value for the energy gap in Mn_{12} was estimated to be 0.74[30] or 1.7 eV.[31] However, the exact determination of the real value of the full energy gap of individual Mn_{12} molecules requires a large set of additional STS measurements upon variation of tunneling conditions. Nonetheless, the good agreement between the present experimental and previous theoretical results on the electronic structure of Mn_{12} indicates that the use of short highly conductive ligands and linker molecules allows the conservation of the molecular electronic structure during the deposition and facilitates direct access to the electronic—and consequently to the magnetic—properties of the Mn_{12} core.

Conclusions

We synthesized and characterized the new Mn_{12} complex **2**·4.4$CHCl_3$. An optimized method using short acidic linker molecules for the wet chemical deposition of Mn_{12} complexes on the Au(111) surface was developed. The method should be widely applicable to Mn_{12} complexes with very different ligand shells. STS measurements revealed the presence of an energy gap in individual Mn_{12} molecules deposited on functionalized Au(111) surfaces that is in reasonable agreement with previous experiments and calculations. The results represent a crucial step toward addressing the magnetic properties of individual Mn_{12} single-molecule magnets by means of scanning tunneling spectroscopy.

Acknowledgment. This work was supported by the Deutsche Forschungsgemeinschaft (DFG) through Sonderforschungsbereich (SFB) 513. We thank M. Bein for the preparation of single crystals and A. Barth for the SQUID measurements.

Supporting Information Available: Synthetic details and characterization data of 4-MOBCA; XPS spectra; X-ray crystallographic data of compound **2** as CIF file. This material is available free of charge via the Internet at http://pubs.acs.org.

JA074884Z